IEEE Access
Multidisciplinary | Rapid Review | Open Access Journal

Date of publication xxxx 00, 0000, date of current version xxxx 00, 0000.

Digital Object Identifier 10.1109/ACCESS.2017.Doi Number

Hybrid Model-Based Fuzzy Logic Diagnostic System for Stator Faults in Three-Phase Cage Induction Motors

Raya A. K. Aswad[1], Bassim M. H. Jassim[1], Member, IEEE, Bashar Zahawi[2], Senior Member, IEEE, and Shady Gadoue[3]

[1]Department of Electrical Engineering, University of Baghdad, Baghdad, Iraq
[2]Advanced Power and Energy Center, Department of Electrical Engineering and Computer Science, Khalifa University, Abu Dhabi 127788, UAE
[3]School of Electronic Engineering and Computer Science, Queen Mary University of London, London E1 4NS, United Kingdom

Corresponding author: Bassim M. H. Jassim (e-mail: bassim.jassim@uob.edu.iq).

ABSTRACT The widespread use of three-phase cage induction motors in so many critical industrial, commercial and domestic applications means that there is a real need to develop online diagnostic systems to monitor the state of the machine during operation. This paper presents a hybrid diagnostic system that combines a model-based strategy with a fuzzy logic classifier to identify abnormal motor states due to single-phasing or inter-turn stator winding faults. Only voltage and current measurements are required to extract the fault symptoms, which are represented as model parameters variations in an equivalent virtual healthy motor, negating the need to use complex models of faulty machines. A trust-region method is used to estimate the machine model parameters, with the final decision on the type, location and extent of the fault being made by the fuzzy logic classifier. The proposed diagnostic system was experimentally verified using a 1.0 hp three-phase test induction motor. Results show that the proposal method can efficiently diagnose single phasing and inter-turn stator winding faults even when operating with unbalanced supply voltages and in the presence of significant levels of measurement noise.

INDEX TERMS Fault diagnosis, fuzzy logic, induction motors, stator faults.

I. INTRODUCTION

Embedding an online, intelligent diagnostic system to monitor the condition of a three-phase induction motor is beneficial for high-value industrial applications in which unexpected shutdowns can be very expensive. Fault diagnosis combines three different tasks: fault detection, isolation, and identification [1]. On detection of an abnormality of some kind, an alarm is raised. Next, the system has to distinguish if the alarm is related to a real issue and is not just an undesired false alarms. After ensuring that a real fault exists, the fault identification stage would provide more information on the type of fault, its severity and location. The diagnostics of induction motor faults is an active and well-established area of research [2], including the identification of open-circuit faults and inter-turn winding faults using a variety of methods such as model-based techniques [3], [4] motor current signature analysis (MCSA) [5], [6], Park vector techniques [7], and knowledge-based strategies [8]. Detection and identification of broken rotor bar faults have also been suggested based on signal analyses methods [9], and more recently on a new technique using the Walsh-Hadamard domain and the k-NN algorithm [10]. Bearings fault diagnosis has long been performed using current signature analysis and knowledge-based strategies [11], [12], and more recently, a tensor-based approach [13]. The use of the Internet of Things for detecting outer and inner ring faults has also been suggested [14]. Diagnostic methods for eccentricity faults have also been developed [15], [16]. In addition to detection strategies for more than one type of induction motor fault [16]-[18].

The most common types of induction motor faults and their frequency of occurrence are as follows: 40-50% of all faults are bearings faults, 30-40% are stator faults and 5-10% are rotor faults [19]. These percentages vary depending on machine size and, according to the literature, stator winding faults occur more frequently in medium and high voltage machines [20]. Hence, this study focuses on induction motor open-circuit and inter-turn short-circuit stator winding faults.

The main symptoms of these faults are critically unbalanced voltages, overheating, excessive vibration, and high current consumption [3], [21]. However, since these symptoms are common to many different types of faults, more tests are required to get an adequate diagnosis. Generally, diagnosis strategies can be divided into three groups: signal-based, model-based, and knowledge-based. One of the most popular signal-based methods is motor current signature analysis in which the fault type is determined from direct analysis of the stator current waveform. MCSA is used to diagnose an inter-turn short circuit fault using Wavelet Transform (WT) in [5]. Although WT provides information in both time and frequency domains, it is sensitive to signal noise. The use of a Kalman filter has been developed as an alternative [22]. Model-based/parameter estimation methods have also been suggested for the diagnosis of stator winding faults. In [23], [24] model parameters are estimated using a stochastic optimization methods and open-circuit fault features are extracted from the obtained values of stator/rotor resistances or the number of turns. While in [3], the estimation of fault loop resistance and the percentage of shorted turns is used as an inter-turn short circuit fault feature, estimated by particle filter, a generic Bayesian filtering approach, which can be applied to nonlinear systems and non- Gaussian noise. Knowledge-based methods in which data corresponding to both healthy and faulty conditions are gathered for different load conditions, then used to train classifications tools for making the final decision on the state of the machine have also been employed for detecting stator short-circuit faults [25], [26]. In general, the signal-based approach is the simplest; however, disturbances affect its accuracy [8]. Some noise immunity can be achieved using model-based or knowledge-based strategies, at the cost of system complexity.

Model-based techniques have been suggested for the purpose of stator winding faults identification [3], [27]-[29]; However, none of these studies examined the effectiveness of utilizing the number of stator winding turns to extract faults' features; i.e., the possibility of employing a model of a machine with asymmetrical windings in which each of the three stator windings has a different number of turns. In this this paper, a model of an asymmetrical induction machine [30] is used as the basis of a reliable hybrid diagnostic system for induction machine stator winding faults. Model parameter values can be easily calculated from general machine parameters without the need for detailed information about motor geometry or winding arrangements. The proposed diagnostic system combines this relatively simple model of an asymmetrical induction motor with a trust-region method analysis and a fuzzy logic classifier to recognize unhealthy conditions and give further details of the fault location and its severity; a matter of great importance for increasing the reliability and effectiveness of any maintenance regime. The proposed diagnostic system is experimentally verified using a 0.75 kW cage induction motor test rig. What's more, the effectiveness of the proposed scheme is tested and verified under practical, non-ideal operating conditions such as unbalanced supply voltages and measurements noise, demonstrating excellent performance characteristics. The contributions of this work can be summarized as follows: 1) The use of a simple model of the machine, eliminating the need for extra equations to represent the various fault conditions. 2) Defining the healthy state by appropriate FL rules instead of initiating the estimation process with pre-specified threshold values to recognize a healthy/faulty state. 3) Recognition of the severity of the inter-turn short-circuit fault. 4) The method is fully tested and verified under practical operating conditions where the effects of an unbalanced supply voltage, load variations, and signal noise are accounted for.

II. THE PROPOSED DIAGNOSTICS SYSTEM

The first step in constructing a diagnostic system is to extract fault features. For each fault type, these features should be unique and capable of specifying the fault type without ambiguity. In this study, the number of stator winding turns are used to extracting the features corresponding to winding open-circuit and inter-turn short-circuit faults. The Trust-Region Method (TRM), which enjoys fast convergence speeds and strong stability [31], is selected for estimating the effective number of turns. TRM is used to minimize the sum of the squared errors between the measured stator currents (i_a, i_b, and i_c) and the corresponding currents calculated from a virtual motor ($i\hat{}_a$, $i\hat{}_b$, and $i\hat{}_c$). The resulting values of machine parameters (rotor and stator resistances, rotor and stator inductances, and mutual inductance) are then used to estimate the effective number of stator winding turns ($N_{as,}$, $N_{bs,}$ and $N_{cs,}$). Finally, a fuzzy logic classifier uses the estimated values of $N_{as,}$, $N_{bs,}$, and $N_{cs,}$ to declare the machine's condition, fault severity, and location. Fig. 1 shows the overall scheme of the suggested diagnostic system.

A. MODEL BASED THEORY

The Model-based approaches have been successfully used for diagnosing faults in different engineering applications. Model-based theory is developed from the traditional hardware redundancy approach, which identifies a component's condition by analyzing the differences between the condition of the component under consideration and an additional hardware component operating in parallel. This hardware redundancy is often replaced by analytical "software" redundancy [32] to reduce system cost and space.

The proposed diagnostic system employs a software model of the motor (a virtual healthy motor) operating in parallel with the machine under examination to generate the required information. Previous approaches used a model of a faulty machine for comparison with the actual motor [3], [27], i.e., a complex model of the machine since redundant equations are needed for faults representation. In contrast, the "virtual healthy motor" adopted in this work is represented in qd-stationary reference frame [30], with consideration to an

asymmetrical induction motors where the number of a stator winding at each phase are not the same ($N_{as,} \neq N_{bs,} \neq N_{cs,}$).

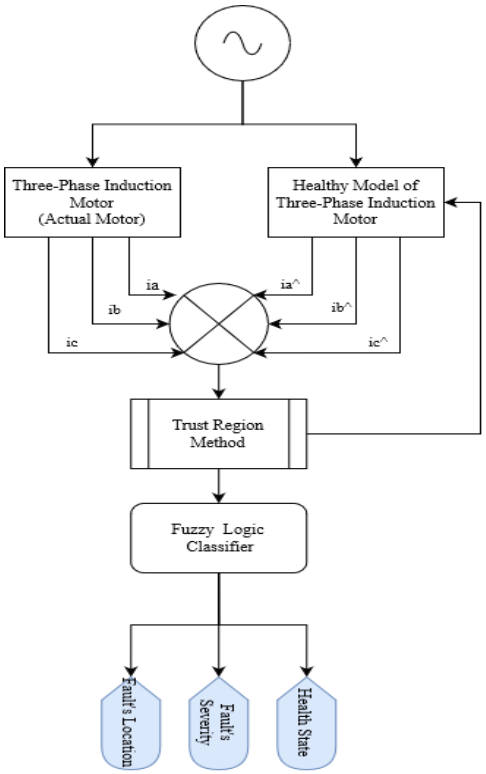

FIGURE 1. **The hybrid model-based/fuzzy logic diagnostic system.**

B. TRUST-REGION METHOD

The Trust-Region Method (TRM) is a numerical (deterministic) optimization method. An objective function f is approximated to a simpler quadratic function m (the standard TRM represents the quadratic function by the first two terms of Taylor's approximation) in which m reflects the behavior of f in a neighborhood (trust-region) around the current point. Several trials are conducted for solving the sub-problem (the quadratic function) until global convergence of the main objective function. The trust-region radius is updated according to the ratio of the expected change in f to the predicted change in m [31]. The TRM process of as follows:

Step 1: Measure the three-phase stator currents (i_a, i_b, i_c) and voltages (v_a,v_b,v_c).

Step 2: Generate the simulated three-phase currents ($i\hat{}_a$, $i\hat{}_b$, $i\hat{}_c$) from the virtual machine using the measured supply voltages data as an input.

Step 3: Evaluate the objective function $f(\boldsymbol{X})$ given by:

$$f(\boldsymbol{X}) = \sum_{j=1}^{N} \{[i_a(k) - i\hat{}_a(k)]^2 + [i_b(k) - i\hat{}_b(k)]^2 + [i_c(k) - i\hat{}_c(k)]^2\} \quad (1)$$

where N is the number of samples. The estimation process is divided into two stages for faster convergence. The model parameters are estimated first and these values are then used in the estimation of the number of turns. Thus, $\mathbf{X}$={R_s, R_r, L_m, L_s, L_r, $LOAD$} at the first stage of the estimation, while $\mathbf{X}$={N_{as}, N_{bs}, N_{cs}} at the second stage of the estimation, where R_s, R_r, L_s, L_r are the stator and rotor resistances and inductances, L_m is the magnetizing inductance and $LOAD$ is the load level.

Step 4: Create an initial circle trust-region with radius Δ, set $\zeta \in [0, 1/4)$

Step 5: Solve the following sub-problem for $k = 0, 1, \ldots$

$$\min_{\|\boldsymbol{d}\| \le \Delta^k} m(\boldsymbol{d})^k = f(\boldsymbol{X})^k + [\nabla f(\boldsymbol{X})^k]^T \boldsymbol{d} + \frac{1}{2} \boldsymbol{d}^T B(\boldsymbol{X})^k \boldsymbol{d} \quad (2)$$

where $\|\boldsymbol{d}\|$ is the second norm of $\boldsymbol{d}$ (the square root of the sum of the squared values) and $B(\boldsymbol{X})$ is the approximate hessian matrix:

$$B(\boldsymbol{X}) = \begin{bmatrix} \frac{\partial^2 f(x)}{\partial^2 ia} & \frac{\partial^2 f(x)}{\partial^2 ia\, ib} & \frac{\partial^2 f(x)}{\partial^2 ia\, ic} \\ \frac{\partial^2 f(x)}{\partial^2 ib\, ia} & \frac{\partial^2 f(x)}{\partial^2 ib} & \frac{\partial^2 f(x)}{\partial^2 ib\, ic} \\ \frac{\partial^2 f(x)}{\partial^2 ic\, ia} & \frac{\partial^2 f(x)}{\partial^2 ic\, ib} & \frac{\partial^2 f(x)}{\partial^2 ic} \end{bmatrix} \quad (3)$$

Step 6: Find the ratio of the actual reduction in the objective function to the predicted reduction (ρ^k)

$$\rho^k = \frac{f(\boldsymbol{X})^k - (f(\boldsymbol{X})^k + \boldsymbol{d}^k)}{m(\boldsymbol{0})^k - m(\boldsymbol{d})^k \boldsymbol{d}^k} \quad (4)$$

for k=0, 1, 2, …

Evaluate ρ^k

if $\rho^k < \frac{1}{4}$

$\Delta^{k+1} = \frac{1}{4}\|\boldsymbol{d}^k\|$

else

if $\rho^k > \frac{3}{4}$ and $\|\boldsymbol{d}^k\| = \Delta^k$

$\Delta^{k+1} = \min(2\Delta^k, \Delta)$

else

$\Delta^{k+1} = \Delta^k$;

if $\rho^k > \zeta$,

$\boldsymbol{X}^{k+1} = \boldsymbol{X}^k + \boldsymbol{d}^k$

else

$\boldsymbol{X}^{k+1} = \boldsymbol{X}^k$

end (for).

Step 7: Check that the termination condition (the function tolerance is less than 0.001) is valid. If so, stop and save the values of {N_{as}, N_{bs}, N_{cs}} else go to **Step 3.**

C. FUZZY LOGIC CLASSIFIER

Fuzzy Logic (FL) is used as a classification tool to make the final decision about the state of the motor. FL has four main stages: fuzzification, rule-building, aggregation, and defuzzification. Crisp input/output values are converted to linguistic variables (fuzzy values) in the fuzzification stage. The link between the input linguistic variables and the output linguistic variables is represented by if-then rules. Rules are combined in the aggregation stage before defuzzification, i.e. converting the linguistic variables to crisp values. An FL-Mamdani type system was developed in Matlab using three inputs (N_{as}, N_{bs}, N_{cs}) and three outputs (state, severity, and

location) as demonstrated in Fig. 2. Input/output variables are represented by simple triangular membership functions to convert the crisp values into fuzzy values. Each input variable has four membership functions: lowest, lower, low, and high. The output state has three fuzzy variables: healthy, open-circuit, and short-circuit. The output severity has three fuzzy variables: low (indicating no fault or an inter-turn fault of 2%), moderate (indicating an inter-turn fault of between 2% and 8%), and high (indicating an open-circuit fault or an inter-turn fault of 8% or higher). Finally, four linguistic variables (phase_a, phase_b, phase_c, and none) represent the output location. Table 1 shows the ranges of these linguistic variables. The total number of rules is 64, written in accordance with simulation and experimental results. Some of these rules are shown below as an example:

1-if (N_{as} is low), (N_{bs} is high) and (N_{cs} is high) then (state is short) (severity is low) (location is phase_a).

2- if (N_{as} is lower), (N_{bs} is high) and (N_{cs} is high) then (state is short) (severity is moderate) (location is phase_a).

3- if (N_{as} is low), (N_{bs} is low) and (N_{cs} is low) then (state is healthy) (severity is low) (location is none).

4- if (N_{as} is low), (N_{bs} is high) and (N_{cs} is low) then (state is open) (severity is high) (location is phase_a).

5- if (N_{as} is low), (N_{bs} is low) and (N_{cs} is high) then (state is open) (severity is high) (location is phase_b).

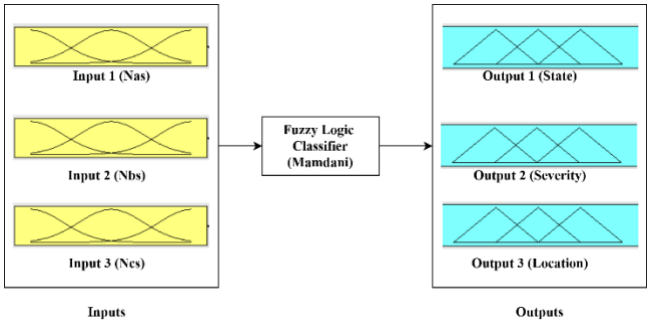

FIGURE 2. Fuzzy logic inputs and outputs.

TABLE I
FL LINGUISTIC VARIABLE RANGE

Variable	Type	Range
lowest	input	[0.7 0.7 0.93]
lower	input	[0.9 0.97 0.99]
low	input	[0.98 1.05 1.07]
high	input	[1.061 1.3 1.3]
healthy	output	[0 0.2 0.4]
short	output	[0.4 0.6 0.8]
open	output	[0.8 1 1.2]
low	output	[0 0.1 0.2]
moderate	output	[0.2 0.3 0.4]
high	output	[0.4 0.5 0.6]
phase_a	output	[0 0.2 0.4]
phase_b	output	[0.4 0.6 0.8]
phase_c	output	[0.8 1 1.2]
none	output	[1.2 1.4 1.6]

III. EXPERIMENTAL INVESTIGATION

A. EXPERIMENTAL TEST RIG

A 0.75kW, 4-pole, 380V three-phase induction motor experimental test rig was constructed for examining the performance of the proposed diagnostic system, as shown in Fig.3. The parameters of the test machine are given in the appendix. A permanent magnet dc generator supplying a resistive load was coupled with the induction motor to provide loading. Three hall-effect voltage sensors (HV25) and three hall-effect current sensors (HTS6) were used to measure the supply voltages and the stator currents. These signals were gathered through a USB Data Acquisition (DAQ) instrument. The DAQ (DI-4208) was interfaced with a (PC) through the USB cable.

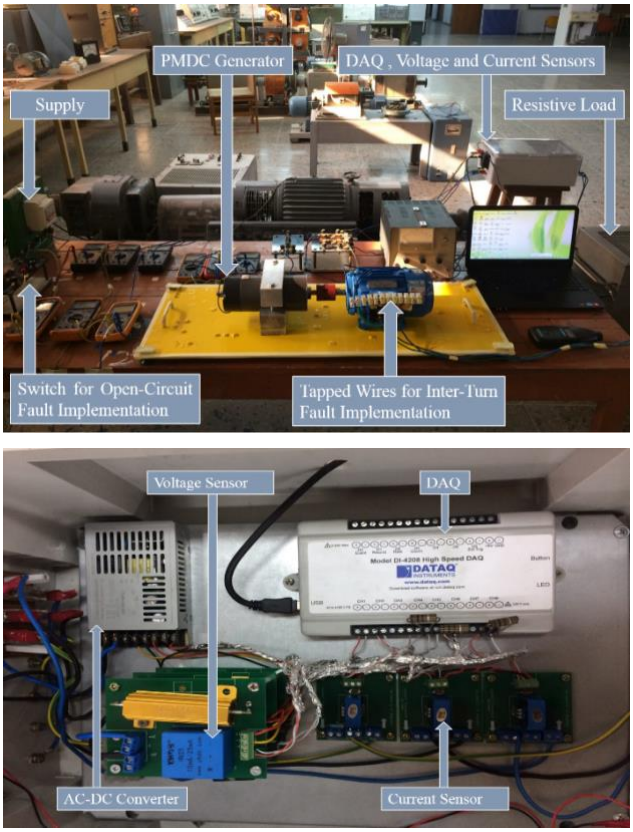

FIGURE 3. Photos of the experimental test rig.

The test induction motor was fed from an inherently unbalanced three-phase voltage supply (the laboratory supply had imbalanced voltages with a voltage unbalance factor (VUF) [34] of up to 5%. The unbalance in the waveforms is due to the unbalanced voltage source and other inherent asymmetries. Three load levels were used during the tests, obtained by adjusting the bank resistances attached to the dc generator. Load level 1 corresponding to a lightly loaded machine, load level 2 corresponding to a load of about 50% of full-load, and load level 3 corresponding to a load of between 70% and 80% of full load. Voltage and current data were collected using WinDaq software for a one-second period at a sampling rate of 1000 S/s. Figs. 4 shows the measured current

waveforms for a healthy condition. Fig. 5 shows the measured current waveforms at load level 1 with phase *a* open-circuited. No current passes through the faulty phase, while the remaining two healthy phases carry significantly elevated values of current. Figs. 6 and 7 show the voltage and current waveforms in the presence of 2% and 10% inter-turn short-circuit fault at phase *a*, respectively. To introduce the inter-turn fault, the motor was rewound, and tapped wires were pull-outed from phase *a* every eight turns, so that 2%, 4%, 6%, 8%, and 10% inter-turn short-circuit faults severity could be obtained. Comparing Fig. 6 with Fig. 7, it is evident that the waveform imbalance is more pronounced with the more severe fault, as would be expected (the current unbalance factor was 11.7% for a 2% inter-turn fault, and 25% for 10% inter-turn fault).

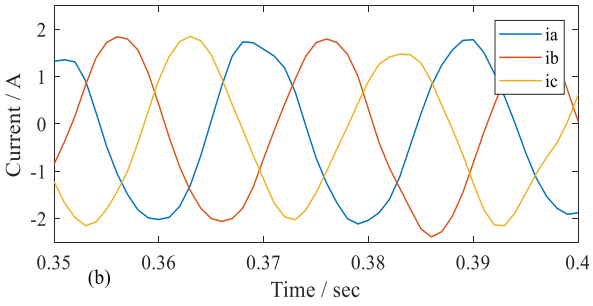

FIGURE 4. **Measured stator current waveforms; Load level 1, healthy condition (1000S/s sampling rate).**

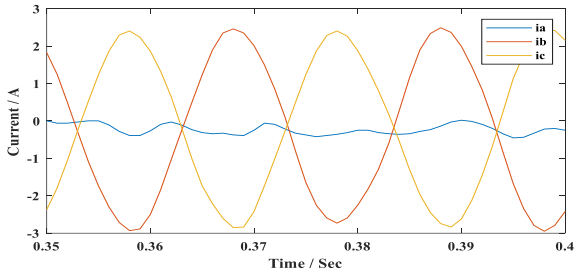

FIGURE 5. **Measured stator current waveforms; Load level 1, open-circuit fault, phase *a* (1000S/s sampling rate).**

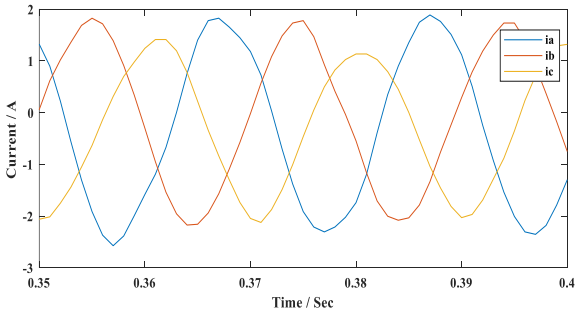

FIGURE 6. **Measured stator current waveforms; Load level 1, 2% inter-turn fault, phase *a* (1000S/s sampling rate).**

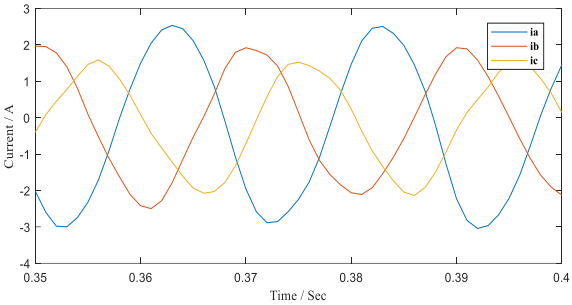

FIGURE 7. **Measured stator current waveforms; Load level 1, 10% inter-turn fault, phase *a* (1000S/s sampling rate).**

A higher sampling rate of 5000 S/s was also used so that the noise immunity of the proposed scheme could be investigated. Figs. 8 and 9 show two examples of these waveforms.

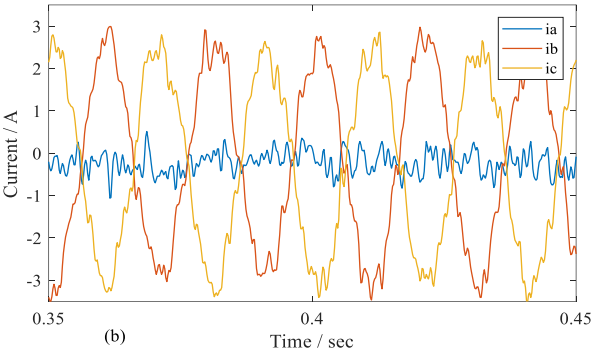

FIGURE 8. **Measured stator current waveforms; Load level 1, open-circuit fault, phase *a* (5000S/s sampling rate).**

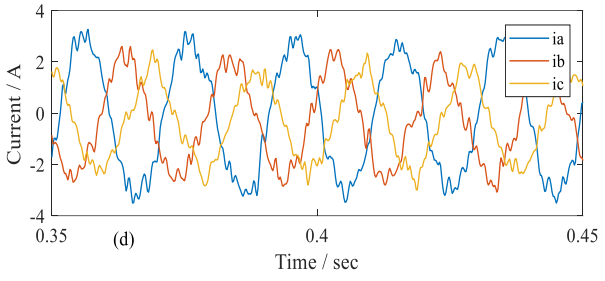

FIGURE 9. **Measured stator current waveforms; Load level 1, 10% inter-turn fault, phase *a* (5000S/s sampling rate).**

IV. ANALYSIS AND RESULTS

Any fault in the machine will affect the effective values of the motor parameters [35] and it is important to consider this in the estimation process. Parameter values are estimated (together with the motor loading condition) at the first stage of the TRM optimization, using the cost function equation (1). which represents the difference between the simulated stator currents of the virtual model (set at full load initially) and the measured stator currents of the motor under examination. The effective values of the stator windings number of turns (N_{as}, N_{bs}, N_{cs}), are then obtained at the second stage of the TRM optimization. The estimation process was implemented in Matlab R2017b/Simulink environment.

The values of the cost function, initially and at the end of each stage of the estimation process, are given in Table 2 for a healthy motor, an open circuit fault and inter-turn faults at various severities. For the healthy motor, the initial value of the cost function is maximum when the motor is at load level 1 since the virtual model is set initially at full load. At the end of the first stage of estimation, the cost function decreases considerably, as the virtual motor catches up the actual operating conditions of the examined motor. The value of the cost function decreases further by the end of the second stage of the estimation process. The initial values of the cost function for the open-circuit fault are higher than the corresponding values for the healthy condition because the current in the faulty phase of the motor is zero, unlike the virtual motor's current at the start of the process. For the inter-turn fault, it can be seen that the initial cost function values go down as the fault severity increases since a higher fault severity means higher values of stator currents and a better match with the initial current of the virtual motor. At the end of the second stage, the cost function values for all conditions are reduced further. Note that the estimation of the load level is higher than the actual loading for all fault conditions as the currents would be higher than their normal values. The open-circuit fault, and the 6% and 10% inter-turn faults, were examined at load level 1 only, because the available current sensors were rated at a maximum of 6 A.

TABLE 2
COST FUNCTION AND ESTIMATED LOAD VALUES (1000 S/S; 5000 S/S)

Operating Condition	Initial (full-load)	End of 1st stage of est.	End of 2nd stage of est.	Est. load level
Healthy (load level 1)	669.5; 2.28e3	71.4; 609.0	69.7; 600.0	11%; 12%
Healthy (load level 2)	243.6; 1.00e3	61.6; 528.8	60.6; 519.7	53%; 58%
Healthy (load level 3)	119.2; 629.3	51.0; 439.6	50.2; 435.6	73%; 81%
o.c. fault (load level 1)	14.0e3; 28.13e3	1.1e3; 4.64e3	1.0e3; 4.46e3	6%; 5%
2% inter-turn fault (load level 1)	573.3; 1.89e3	75.5; 619.5	65.3; 600.3	25%; 27%
2% inter-turn fault (load level 2)	233.5; 785.3	73.3; 497.4	66.1; 471.5	58%; 71%
2% inter-turn fault (load level 3)	99.1; 555.8	55.3; 431.8	49.1; 414.6	81%; 94%
6% inter-turn fault (load level 1)	423.7; 1.42e3	98.8; 580.8	59.0; 477.0	36%; 38%
10% inter-turn fault (load level 1)	317.3; 1.13e3	121.8; 628.2	51.5; 443.5	47%; 51%

The estimated normalized values of $N_{as,}$, $N_{bs,}$, and $N_{cs,}$ for the healthy and faulty motor conditions are shown in Table 3 together with the corresponding fuzzy logic results. Normalized values were used (1 pu) to generalize the fuzzy rules for all motor sizes. As shown, the values of these parameters vary in accordance with the motor's state, the location of the fault, and its severity. As evident from the results, the noisy environment (i.e. when using the increased sampling rate of 5000S/s) does not have much of an effect on the accuracy of the results.

V. CONCLUSION

A hybrid diagnostic system for winding faults in three-phase cage induction motors is presented in this paper. The proposed scheme combines a model-based strategy with fuzzy logic (FL) to identify the type, location and severity of stator winding faults. The main part of the diagnostic system is feature extraction, carried out using the trust-region method. This was used to estimate the corresponding variation in the number of turns of the virtual motor. A FL classifier then uses the extracted features to announce the motor's health condition (healthy, faulty with open-circuit fault, and faulty with inter-turn fault), fault's severity, and location.

The proposed diagnostics system considers the healthy state as an unknown condition, evaluated by the FL classifier, removing the need to set threshold parameter values for separating the healthy state, as is usually the case. The system is not dependent on motor size and can operate successfully in the presence of noise, at different loading conditions, and even with a significantly unbalanced supply. It is also non-intrusive and requires only terminal voltage and current measurements. All the above features were experimentally verified using a 0.75 kW induction motor test rig (which was re-wound to allow the introduction of inter-turn short circuit faults of different severities). Other faults like broken rotor bars, eccentricity faults and bearings faults are not considered in this work.

TABLE 3
FUZZY LOGIC RESULTS (1000 S/S; 5000 S/S)

Operating Condition	FL inputs (N_{as}, N_{bs}, N_{cs})	FL outputs	Estimation (state, severity, location)
Healthy (load level 1)	1.02, 0.98, 1.01; 1.02, 0.99, 1.00	0.6, 0.1, 0.6; 0.59, 0.1, 0.63	(healthy, low, none)
Healthy (load level 2)	1.02, 0.99, 1.01; 1.01, 0.99, 1.00	0.2, 0.1, 1.4; 0.2, 0.1, 1.4	(healthy, low, none)
Healthy (load level 3)	1.02, 0.99, 1.00; 1.03, 1.0, 1.01	0.2, 0.1, 1.4; 0.2, 0.1, 1.4	(healthy, low, none)
o.c. fault phase *b* (load level 1)	0.97, 1.01, 1.20; 0.98, 1.00, 1.23	1.0, 0.5, 0.6; 1.0, 0.5, 0.6	(open, high, phase *b*)
2% inter-turn fault phase *a* (load level 1)	0.96, 1.00, 1.05; 0.97, 0.99, 1.04	0.6, 0.3, 0.2; 0.6, 0.3, 0.2	(short, moderate, phase *a*)
2% inter-turn fault phase *a* (load level 2)	0.98, 1.00, 1.05; 0.98, 1.00, 1.06	0.6, 0.3, 0.2; 0.6, 0.3, 0.2	(short, moderate, phase *a*)

2% inter-turn fault phase *a* (load level 3)	0.98, 1.0, 1.06; 0.98, 1.01, 1.06	0.56, 0.28, 0.3; 0.6, 0.3, 0.2	(short, moderate, phase *a*)
4% inter-turn fault phase *a* (load level 1)	0.94, 1.0, 1.06; 0.95, 1.0, 1.06	0.6, 0.3, 0.2; 0.6, 0.3, 0.2	(short, moderate, phase *a*)
4% inter-turn fault phase *a* (load level 2)	0.95, 1.0, 1.06; 0.96, 1.02, 1.0	0.6, 0.3, 0.2; 0.6, 0.3, 0.2	(short, moderate, phase *a*)
4% inter-turn fault phase *a* (load level 3)	0.96, 1.02, 1.0; 0.94, 1.00, 1.04	0.6, 0.5, 0.2; 0.6, 0.3, 0.2	(short, moderate, phase *a*)
6% inter-turn fault phase *a* (load level 1)	0.91, 1.0, 1.06; 0.92, 1.0, 1.07	0.6, 0.4, 0.2; 0.79, 0.5, 0.4	(short, high, phase *a*)
10% inter-turn fault phase *a* (load level 1)	0.86, 1.0, 1.07; 0.88, 1.0, 1.09	0.6, 0.5, 0.2; 0.6, 0.5, 0.2	(short, high, phase *a*)

APPENDIX

The parameters of the 0.75kW, 380V, 50 Hz, 4-pole three-phase test induction motor used in the investigation are as follows: rated current = 1.88 A, coils per phase = 2, turns per phase = 192, stator resistance = 14.56 Ω, stator reactance = 14.28 Ω, magnetizing reactance = 151.5 Ω, rotor resistance = 11.83 Ω, and rotor reactance = 14.28 Ω.

ACKNOWLEDGMENT

The authors wish to thank the staff of the AC Lab at the department of Electrical Engineering, University of Baghdad, for their efforts in setting up the experimental test rig used in this investigation.

REFERENCES

[1] Z. Gao, C. Cecati, and S. X. Ding, "A survey of fault diagnosis and fault-tolerant techniques- Part I: fault diagnosis with model-based and signal-based approaches," *IEEE Trans Ind. Electron.*, vol. 62, no. 6, pp. 3757–3767, 2015.

[2] M. E. E. -D. Atta, D. K. Ibrahim and M. I. Gilany, "Broken Bar Fault Detection and Diagnosis Techniques for Induction Motors and Drives: State of the Art," in IEEE Access, vol. 10, pp. 88504-88526, 2022, doi: 10.1109/ACCESS.2022.3200058.

[3] V. Nguyen, J. Seshadrinath, D. Wang, S. Nadarajan, and V. Vaiyapuri, "Model-Based Diagnosis and RUL Estimation of Induction Machines Under Interturn Fault," *IEEE Trans. Ind. Appl.*, vol. 53, no. 3, pp. 2690–2701, 2017.

[4] J. Huang, Y. Liu, and Z. Liang, "Rapid evaluation of the mechanical fault severity in induction motors using the model-based diagnosis technique," *IET Elect. Power Appl.*, vol. 15, no. 2, pp. 145-158, Feb. 2021.

[5] A. K. Verma, S. Radhika and S. V. Padmanabhan, "Wavelet Based Fault Detection and Diagnosis Using Online MCSA of Stator Winding Faults Due to Insulation Failure in Industrial Induction Machine," 2018 IEEE Recent Advances in Intelligent Computational Systems (RAICS), 2018, pp. 204-208, doi: 10.1109/RAICS.2018.8635058.

[6] V. Aviña-Corral, J. Rangel-Magdaleno, C. Morales-Perez and J. Hernandez, "Bearing Fault Detection in Adjustable Speed Drive-Powered Induction Machine by Using Motor Current Signature Analysis and Goodness-of-Fit Tests," *IEEE Transactions on Industrial Informatics*, vol. 17, no. 12, pp. 8265-8274, Dec. 2021, doi: 10.1109/TII.2021.3061555.

[7] F. Husari and J. Seshadrinath, "Inter-Turn Fault Diagnosis of Induction Motor Fed by PCC-VSI Using Park Vector Approach," 2020 IEEE International Conference on Power Electronics, Drives and Energy Systems (PEDES), 2020, pp. 1-6, doi: 10.1109/PEDES49360.2020.9379388.

[8] A. Mejia-Barron, J. de Santiago-Perez, D. Granados-Lieberman, J. Amezquita-Sanchez, and M. Valtierra-Rodriguez, "Shannon Entropy Index and a Fuzzy Logic System for the Assessment of Stator Winding Short-Circuit Faults in Induction Motors," *Electronics*, vol. 8, no. 1, p. 90, Jan. 2019, doi: 10.3390/electronics8010090.

[9] I. Zamudio-Ramírez et al., "Automatic Diagnosis of Electromechanical Faults in Induction Motors Based on the Transient Analysis of the Stray Flux via MUSIC Methods," in IEEE Transactions on Industry Applications, vol. 56, no. 4, pp. 3604-3613, July-Aug. 2020, doi: 10.1109/TIA.2020.2988002.

[10] M. Lopez-Ramirez, C. Rodriguez-Donate, L. M. Ledesma-Carrillo, F. J. Villalobos-Pina, J. U. Munoz-Minjares and E. Cabal-Yepez, "Walsh–Hadamard Domain-Based Intelligent Online Fault Diagnosis of Broken Rotor Bars in Induction Motors," in IEEE Transactions on Instrumentation and Measurement, vol. 71, pp. 1-11, 2022, Art no. 3505511, doi: 10.1109/TIM.2022.3141152.

[11] J. Xie, Z. Li, Z. Zhou and S. Liu, "A Novel Bearing Fault Classification Method Based on XGBoost: The Fusion of Deep Learning-Based Features and Empirical Features," in IEEE Transactions on Instrumentation and Measurement, vol. 70, pp. 1-9, 2021, Art no. 3506709, doi: 10.1109/TIM.2020.3042315.

[12] S. M. K. Zaman, X. Liang and L. Zhang, "Greedy-Gradient Max Cut-Based Fault Diagnosis for Direct Online Induction Motors," in IEEE Access, vol. 8, pp. 177851-177862, 2020, doi: 10.1109/ACCESS.2020.3027322.

[13] J. Martinez-Roman, R. Puche-Panadero, A. Sapena-Bano, C. Terron-Santiago, J. Burriel-Valencia, and M. Pineda-Sanchez, "Analytical Model of Induction Machines with Multiple Cage Faults Using the Winding Tensor Approach," *Sensors*, vol. 21, no. 15, p. 5076, Jul. 2021, doi: 10.3390/s21155076.

[14] M. -Q. Tran, M. Elsisi, K. Mahmoud, M. -K. Liu, M. Lehtonen and M. M. F. Darwish, "Experimental Setup for Online Fault Diagnosis of Induction Machines via Promising IoT and Machine Learning: Towards Industry 4.0 Empowerment," in IEEE Access, vol. 9, pp. 115429-115441, 2021, doi: 10.1109/ACCESS.2021.3105297.

[15] R. S. C. Pal and A. R. Mohanty, "A Simplified Dynamical Model of Mixed Eccentricity Fault in a Three-Phase Induction Motor," in IEEE Transactions on Industrial Electronics, vol. 68, no. 5, pp. 4341-4350, May 2021, doi: 10.1109/TIE.2020.2987274.

[16] G. R. Agah, A. Rahideh, H. Khodadadzadeh, S. M. Khoshnazar and S. Hedayatikia, "Broken Rotor Bar and Rotor Eccentricity Fault Detection in Induction Motors Using a Combination of Discrete Wavelet Transform and Teager–Kaiser Energy Operator," in IEEE Transactions on Energy Conversion, vol. 37, no. 3, pp. 2199-2206, Sept. 2022, doi: 10.1109/TEC.2022.3162394.

[17] M. -Q. Tran, M. -K. Liu, Q. -V. Tran and T. -K. Nguyen, "Effective Fault Diagnosis Based on Wavelet and Convolutional Attention Neural Network for Induction Motors," in IEEE Transactions on Instrumentation and Measurement, vol. 71, pp. 1-13, 2022, Art no. 3501613, doi: 10.1109/TIM.2021.3139706.

[18] S. B. Jiang, P. K. Wong, R. Guan, Y. Liang and J. Li, "An Efficient Fault Diagnostic Method for Three-Phase Induction Motors Based on Incremental Broad Learning and Non-Negative Matrix Factorization," in IEEE Access, vol. 7, pp. 17780-17790, 2019, doi: 10.1109/ACCESS.2019.2895909.

[19] C. Terron-Santiago, J. Martinez-Roman, R. Puche-Panadero, and A. Sapena-Bano, "A Review of Techniques Used for Induction Machine Fault Modelling," *Sensors (Basel)*, vol. 21, no. 14:4855, July 2021, doi: 10.3390/s21144855.

[20] K. Gyftakis, P. Panagiotou, and D. Spyrakis, "Detection of simultaneous mechanical faults in 6-kV pumping induction motors using combined MCSA and stray flux methods," *IET Electr. Power Appl.*, vol. 15, no. 5, pp. 643–652, May 2021, doi: 10.1049/elp2.12054.

[21] H. Keskes, A. Braham, and Z. Lachiri, "Broken rotor bar diagnosis in induction machines through stationary wavelet packet transform and multiclass wavelet SVM," *Electr. Power Syst. Res.*, vol. 97, pp. 151–157, April 2013, doi: 10.1016/j.epsr.2012.12.013.
[22] A. Namdar, H. Samet, M. Allahbakhshi, M. Tajdinian, and T. Ghanbari, "A robust stator inter-turn fault detection in induction motor utilizing Kalman filter-based algorithm," *Measurement*, vol. 187, 110181, Jan. 2022, doi: 10.1016/j.measurement.2021.110181.
[23] R. Aswad and B. Jassim, "Open-circuit fault diagnosis in three-phase induction motor using model-based technique," *Arch. Electr. Eng.*, vol. 69, no. 4, pp. 815–827, Nov. 2020, doi: 10.24425/aee.2020.134632.
[24] S. A. Ethni, B. Zahawi, D. Giaouris, and P. P. Acarnley, "Comparison of Particle Swarm and Simulated Annealing Algorithms for Induction Motor Fault Identification," in *Proc. IEEE Conf. Ind. Inf., 2009,* pp. 470–474.
[25] S. B. Jiang, P. K. Wong, R. Guan, Y. Liang and J. Li, "An Efficient Fault Diagnostic Method for Three-Phase Induction Motors Based on Incremental Broad Learning and Non-Negative Matrix Factorization," *IEEE Access*, vol. 7, pp. 17780-17790, Jan. 2019, doi: 10.1109/ACCESS.2019.2895909.
[26] H. Nakamura and Y. Mizuno, "Method for Diagnosing a Short-Circuit Fault in the Stator Winding of a Motor Based on Parameter Identification of Features and a Support Vector Machine," *Energies*, vol. 13, no. 9, p. 2272, May 2020, doi: 10.3390/en13092272.
[27] F. Duan and R. Živanović, "Condition Monitoring of an Induction Motor Stator Windings Via Global Optimization Based on the Hyperbolic Cross Points," in IEEE Transactions on Industrial Electronics, vol. 62, no. 3, pp. 1826-1834, March 2015, doi: 10.1109/TIE.2014.2341563.
[28] A. M. Alturas, S. M. Gadoue, B. Zahawi and M. A. Elgendy, "On the Identifiability of Steady-State Induction Machine Models Using External Measurements," in IEEE Transactions on Energy Conversion, vol. 31, no. 1, pp. 251-259, March 2016, doi: 10.1109/TEC.2015.2460456.
[29] H. Abdallah and B. Kouadri, "On -Line Stator Winding Inter -Turn Short -Circuits Detection in Induction Motors Using Recursive Levenberg -Marquardt Algorithm," *International Journal on Electrical Engineering and Informatics*, vol. 9, pp. 42-57, March 2017, doi: 10.15676/ijeei.2017.9.1.3.
[30] M. Arkan, D. Kostic-perovic, and P. J. Unsworth, "Modelling and simulation of induction motors with inter-turn faults for diagnostics," *Electr. Power Syst. Res.*, vol. 75, no. 1, pp. 57–66, July 2005, doi.org/10.1016/j.epsr.2004.08.015.
[31] P. Wang, L. Shi, Y. Zhang, Y. Wang, and L. Han, "Broken Rotor Bar Fault Detection of Induction Motors Using a Joint Algorithm of Trust Region and Modified Bare-bones Particle Swarm Optimization," *Chin. J. Mech. Eng.* Vol. 32, 10, Feb. 2019, doi.org/10.1186/s10033-019-0325-y.
[32] C. Skliros, M. Esperon Miguez, A. Fakhre, and I Jennions, "A review of model based and data driven methods targeting hardware systems diagnostics." *Diagnostyka*, vol. 20, no. 1, pp. 3-21, 2019, doi:10.29354/diag/99603.
[33] J. Nocedal and S. J. Wright, *Numerical Optimization*, 2nd ed. New York: Springer, 2006.
[34] M. Anwari and A. Hiendro, "New Unbalance Factor for Estimating Performance of a Three-Phase Induction Motor With Under- and Overvoltage Unbalance," *IEEE Trans. ENERGY Convers.*, vol. 25, no. 3, pp. 619–625, 2010.
[35] M. Vedova, A. Germanà, P. Berri, and P. Maggiore, "Model-Based Fault Detection and Identification for Prognostics of Electromechanical Actuators Using Genetic Algorithms," *Aerospace*, vol. 6, no. 94, pp. 1–15, 2019.

Raya A. K. Aswad received her B.Sc. degree in Electrical Engineering from University of Baghdad, Baghdad, Iraq, in 2016 and the M.Sc. degree in Electrical Engineering (Power and Machines) from the same university in 2020.

She is currently working as a quality control engineer for Al-Handasya Electrical Industries Company, Baghdad, Iraq, a partner company licensed by Schneider Electric. Her research interests include fault diagnosis in electrical machines, condition monitoring, and optimization methods.

Bassim M. H. Jassim (M'11) received the B.Sc. and M.Sc. degrees in electrical engineering from the University of Baghdad, Baghdad, Iraq, in 1989 and 1996, respectively, and the Ph.D. degree in electrical engineering from Newcastle University, Newcastle upon Tyne, U.K., in 2014.

From 1989 to 1991, he was a Research Engineer with the commission of research and development at the Ministry of Industry, Baghdad, Iraq. From 1996 to 2001, he was a Researcher with the State Company for Electronic Systems, Baghdad. Since 2001, he has been with the Department of Electrical Engineering, University of Baghdad, where he is currently a Lecturer. His research interests include fault diagnosis, converter design and control, parallel converter operation, and power factor regulation.

Bashar Zahawi (M'96-SM'04) received his BSc and PhD degrees in electrical and electronic engineering from Newcastle University, Newcastle upon Tyne, UK, in 1983 and 1988, respectively.

From 1988 to 1993 he was a design engineer with a U.K. manufacturer of large variable speed drives and other power conversion equipment. He was appointed as a Lecturer in electrical engineering at the University of Manchester, Manchester, U.K. in 1994 and was a Senior Lecturer with the School of Electrical and Electronic Engineering, Newcastle University, Newcastle upon Tyne, U.K. from 2003 to 2014. Since 2014, he has been with the Department of Electrical and Computer Engineering, Khalifa University, Abu Dhabi, United Arab Emirates, where he is currently Professor of electrical power engineering. His research interests include, power conversion, renewable energy, and the application of nonlinear dynamical methods to electrical circuits and systems.

Dr Zahawi is a recipient of the Crompton Premium awarded by the Institution of Electrical Engineers, U.K., and the Denny Medal awarded by the Institute of Marine Engineering, Science & Technology (IMarEST). He is past Chairman of the IEEE Power & Energy Society United Arab Emirates Chapter.

Shady Gadoue received the BSc (Hons) and MSc degrees in Electrical and Electronic Engineering from Alexandria University, Egypt and the PhD degree from Newcastle University, Newcastle upon Tyne, UK in 2009, in the area of Power Electronics and Control Systems.

In 2011, he joined the Electrical Power Research Group at Newcastle University, as a Lecturer. In 2016, he was with the Power and Control Research group at Imperial College London as a full time visiting research scholar. In 2017, he joined the School of Engineering and Applied Science, Aston University, Birmingham, UK, as a Senior Lecturer. Dr. Gadoue is currently with the School of Electronic Engineering and Computer Science at Queen Mary University of London as Associate Professor in Electrical and Electronic Engineering. His research interests include Electrification systems in Transport and Energy, Power Electronics and control systems for electrical vehicles drives powertrain and Batteries for traction applications.